R. Bras. Zootec., 52:e20220082, 2023
https://doi.org/10.37496/rbz5220220082

Non-ruminants
Full-length research article

Revista Brasileira de Zootecnia

Brazilian Journal of Animal Science
e-ISSN 1806-9290
www.rbz.org.br

Morphology, histology, and proteomics of the testicle and epididymis of European quail fed calcium anacardate

Rafael de Sousa Ferreira[1]*, Fábio Roger Vasconcelos[1], Nhaira Maia Vilarinho[1], Emilio de Castro Miguel[2], Ednardo Rodrigues Freitas[1], Arele Arlindo Calderano[3], Luiz Fernando Teixeira Albino[3], Arlindo de Alencar Araripe Noronha Moura[1]

[1] Universidade Federal do Ceará, Departamento de Zootecnia, Fortaleza, CE, Brasil.
[2] Universidade Federal do Ceará, Departamento de Engenharia Metalúrgica e de Materiais, Fortaleza, CE, Brasil.
[3] Universidade Federal de Viçosa, Departamento de Zootecnia, Viçosa, MG, Brasil.

***Corresponding author:**
faelherreira@hotmail.com

Received: June 10, 2022
Accepted: July 14, 2023

How to cite: Ferreira, R. S.; Vasconcelos, F. R.; Vilarinho, N. M.; Miguel, E. C.; Freitas, E. R.; Calderano, A. A.; Albino, L. F. T. and Moura, A. A. A. N. 2023. Morphology, histology, and proteomics of the testicle and epididymis of European quail fed calcium anacardate. Revista Brasileira de Zootecnia 52:e20220082. https://doi.org/10.37496/rbz5220220082

ABSTRACT - This report examines the effects of calcium anacardate (CA) on the morphology, histology, and proteomics of the testes and epididymal ducts of breeding quail. To that end, 22 140-day-old males were grouped in four treatments, each with different concentrations of CA: 0% (control), 0.25%, 0.50%, and 0.75%. The testicles of the animals were weighed and measured, and proteins from the testicles were separated by 1D SDS-PAGE and analyzed via mass spectrometry. Overall, 35 bands were identified in the testicular tissue gels of European quail. Of these, 13 were significantly different, with treatment 0.75% CA being different from the control in all bands. Significant differences among the mean heights of the seminiferous epithelium and diameters of the epididymal duct were observed. In the control group, the average height of the seminiferous epithelium was 71.2 µm, and in 0.75% CA, it was 45.6 µm. Supplementing feed with CA altered the expression of specific proteins, such as superoxide dismutase and heat shock proteins, of the seminal plasma of quail, in addition to facilitating histological alterations regarding the height of the seminiferous epithelium and the diameter of the epididymal duct, improving the reproductive parameters.

Keywords: *Coturnix coturnix*, oxidative stress, poultry, reproduction

1. Introduction

Quail farming has become a viable activity due to several factors such as animal dual purpose (meat and eggs), excellent meat flavor, low implantation costs, and rapid growth and development, providing a swift return on investment for producers (Silva et al., 2009). However, some factors, such as heat stress, can result in oxidative stress, thereby affecting the productivity indices of the birds. Exposure to oxidative stress results in the action of free radicals on the unsaturated lipids of the cell membrane, culminating in cell death (Barreiros, 2006). As a result, there is an overload of reactive oxygen species (ROS) in the body, resulting in damage to the sperm cells, inducing a process known as lipid peroxidation, causing DNA damage and apoptosis, thus decreasing quail fertility (Costa and Streit Jr, 2019).

One way to decrease the harmful effects of free radicals and, consequently, lipid peroxidation is the use of antioxidants, which are substances capable of interrupting the oxidizing action of free radicals, such as nitric oxide and hydroxyl radicals (Bianchi and Antunes, 1999), reducing the negative effects on

reproduction (Aitken and Roman, 2008; Agarwal et al., 2021; Malmir et al., 2021). Factors such as high relative humidity, diseases, vaccinations, temperature variations, heavy metals, poor feed quality, and mycotoxins increase the demand for antioxidant agents, which, if insufficient, cause ROS formation and accumulation (Wang et al., 2009).

Calcium anacardate (CA) is a phenolic compound obtained during the isolation of anacardic acid from cashew nut shell liquid (CNSL) (Paramashivappa et al., 2001). It is a dark, oily, viscous liquid that can be extracted from different parts of the cashew tree (*Anacardium occidentale* L.) (Abreu et al., 2015) and is composed of a mixture of anacardic acid, cardanol, cardol, and methyl cardol (Hamad and Mubofu, 2015). It has several biological functions, such as antibacterial, antitumor, and antioxidant activity (Abreu et al., 2015; Hamad and Mubofu, 2015). As an antioxidant, CA acts by preventing transition metal ions from starting the oxidation process, inactivating oxidation intermediates, and inhibiting various pro-oxidant enzymes (Kubo et al., 2006).

In this study, we hypothesized that CA can reduce the negative effects of oxidative stress in quail reproduction. Thus, the objective of this study was to evaluate the effects of dietary CA supplementation on the morphological, histological, and proteomic characteristics of the testis and epididymis of male quail used for breeding.

2. Material and Methods

2.1. Ethics

The Institutional Animal Care and Use Committee approved all animal handling procedures (case number CEUA/UFC/255225-718/2018), and the experiment was conducted according to the experimental protocol for the use of live birds from the Brazilian College of Animal Experimentation.

2.2. Birds, experimental design, and diet

The experiment was conducted in Fortaleza, CE, Brazil (3°43'6" S, 38°32'36" O). Overall, 22 male quail (*Coturnix coturnix coturnix*) were raised until 140 days of age with *ad libitum* access to feed and water. At 140 days, the birds were weighed and allocated to four treatments and six repetitions in a completely randomized manner: treatment 1 (six animals), treatment 2 (six animals), treatment 3 (five animals), and treatment 4 (five animals). Treatments were formulated by the addition of three different CA levels. In treatment 1 (control group), the diets were not supplemented with CA. In treatments 2, 3, and 4, 0.25%, 0.50%, and 0.75% of calcium anacardate, respectively, were added to the feed over an experimental period of 210 days. Calcium anacardate was extracted from cashew nut liquid through precipitation, according to the methodology adapted from Paramashivappa et al. (2001). Males were raised together with five females in a conventional shed in cages measuring 35 × 25 × 20 cm (length, width, and diameter), equipped with a linear trough feeder, nipple drinker, and egg tray. The experimental diets were formulated to be isonutritive according to the nutritional requirements presented by Silva (2009), and the nutritional and energy composition values of the ingredients were considered according to Rostagno et al. (2017). There was a replacement of the inert according to the inclusion of CA in the proportion of each treatment (Table 1). Calcium from CA was not considered. The animals were subjected to 16 h light per day. After the experimental period, the animals were sacrificed by exsanguination in compliance with the guidelines established by the National Council for Animal Experimentation Control (CONCEA, 2015) and weighed. After weighing, all birds were placed in supine position for posterior incisions in the ventral region for collection of the testes and epididymis. The epididymis was dissected from the testicles before weighing. The left and right testes were weighted and measured (length, diameter, and volume). Testicular volume was calculated using Bissonett's formula, $4/3\ \pi ab^2$ (in which a = half of the long axis and b = half of the short axis), and averaged (Chaturvedi and Bhatt, 1990; Chaturvedi et al., 1993). The testicular gonadosomatic index was calculated using the equation (testis weight/final body weight) × 100%. Samples of the testes and epididymis tissue were reserved for proteomic and histological analysis.

Table 1 - Percentages of ingredients and calculated nutritional composition of the experimental diets used for quail

Ingredient (%)	Calcium anacardate level (%)			
	0 (control)	0.25	0.50	0.75
Corn grain	41.050	41.050	41.050	41.050
Soybean meal	40.790	40.790	40.790	40.790
Calcitic limestone	7.550	7.550	7.550	7.550
Soybean oil	6.600	6.600	6.600	6.600
Dicalcium phosphate	1.670	1.670	1.670	1.670
L-threonine	0.07	0.07	0.07	0.07
L-lysine HCl 78.5%	0.05	0.05	0.05	0.05
DL-methionine 99%	0.270	0.270	0.270	0.270
Inert	1.250	1.000	0.750	0.500
Calcium anacardate[3]	0.000	0.250	0.500	0.750
Salt	0.550	0.550	0.550	0.550
Vitamin supplement[1]	0.100	0.100	0.100	0.100
Mineral supplement[2]	0.050	0.050	0.050	0.050
Total	100.00	100.00	100.00	100.00
Calculated nutritional composition				
Metabolizable energy (kcal/kg)	2,800	2,800	2,800	2,800
Crude protein (%)	21.00	21.00	21.00	21.00
Calcium	3.00	3.00	3.00	3.00
Available phosphorus (%)	0.300	0.300	0.300	0.300
Digestible lysine (%)	1.100	1.100	1.100	1.100
Digestible methi + cystine (%)	0.700	0.700	0.700	0.700
Digestible methionine (%)	0.419	0.419	0.419	0.419
Digestible threonine (%)	0.870	0.870	0.870	0.870

[1] Composition per kg of product: vitamin A, 9,000,000.00 UI; vitamin D3, 2,500,000.00 UI; vitamin E, 20,000.00 Mg; vitamin K3, 2,500.00 mg; vitamin B1, 2,000.00 mg; vitamin B2, 6,000.00 mg; vitamin B12, 15.00 mg; niacin, 35,000.00 mg; pantothenic acid, 12,000.00 mg; vitamin B6, 8,000.00 mg; folic acid, 1,500.00 mg; selenium, 250.00 mg; biotin, 100.00 mg.
[2] Composition per kg of product: iron, 100,000.00 mg; copper, 20.00 g; manganese, 130,000.00 mg; zinc, 130,000.10 mg; iodine, 2,000.00 mg.
[3] Calcium anacardate was extracted according to the methodology adapted from Paramashivappa et al. (2001).

2.3. Proteomics analysis

The testicles used for proteomics were frozen in liquid nitrogen and lyophilized at −55 °C for 24 h, with a minimum pressure of 60 mTorr. For the extraction of proteins, 10 mg of lyophilized sample was diluted in 500 µL of lysis solution (Triton X-100 0.1%) and stored at 4 °C for 1 h, with homogenization conducted at 15-min intervals. Subsequently, 400 µL of sample buffer was added to the samples, followed by sonication for 1 h. The samples were centrifuged at 12,000 × *g* for 30 min at 4 °C, and the supernatant was collected for protein quantification using Bradford's method (Bradford, 1976). The proteins extracted from the testicles were separated by the 1D SDS-PAGE method based on the protocol described by Souza et al. (2020), with modifications. After the run, the gels were stained using Coomassie's Brilliant Blue solution for 12 h and then discolored with methanol and acetic acid solution (40%:10%). The gels were subsequently digitized using the ImageScanner III (GE Healthcare, Piscataway, NJ, USA) and saved in TIFF format, followed by analysis using the Quantity One Software® version 4.6.3 (Bio-Rad, Rockville, MD, USA).

The bands were cut into pieces of approximately 1 mm^3, and tryptic digestion was performed according to De Lazari et al. (2019). Tryptic peptides were separated on a BEH300 C18 column (100 µm × 100 mm) using the nanoAcquity™ system (Waters, USA) and eluted at 600 µL/min with an acetonitrile gradient (5–85%) containing 0.1% formic acid. The liquid chromatography system was connected to a nanoelectrospray mass spectrometry source (SYNAPT HDMS system, Waters, Milford, MA, USA), and mass spectrometry was operated in positive mode at 90 °C and a capillary voltage of 3.5 kV. The instrument was calibrated with fragments of the protonated double ion (phosphoric acid, m/z 686.8461), and the blocking mass used during data-dependent acquisition (DDA), selecting

the precursor MS/MS ions double- or triple-charged. The LC-MS/MS procedure was carried out according to the data-dependent acquisition method (DDA), selecting the double- or triple-charged percussion ions MS/MS. Ions were fragmented by collision-induced dissociation, using argon as the collision gas and a ramp collision energy that varied according to the charge state of the selected precursor ion. Data acquisition was carried out in an m/z interval of 300 to 2,100 for the survey MS (1 scan/s) and an m/z interval of 50 to 2,500 for MS/MS. Data were collected using the MassLynx 4.1 software, processed using Protein Lynx Global Server 2.4 (Waters Corp. Milford, MA, USA), and converted to peak list text files for database searching (.pkl). The Mascot platform (Matrix Science, London, United Kingdom, v. 2.6) was then used to search the NCBIprot and SwissProt database, carrying out gene ontology with the aid of the software for researching protein annotations (STRAP v. 1.5.0.0) and using the UniProtKB database to obtain the terms of the genetic ontology (biological process, molecular function, and cellular component).

Protein-protein networks were retrieved from the STRING database (http://string-db.org) version 10.0 (Viana et al., 2018; Snel et al., 2000), which consists of known and predicted protein interactions collected from direct (physical) and indirect (functional) associations. This database quantitatively integrates interaction data from four sources-genomic context, high-throughput experiments, co-expression, and data from previous publications. The network analysis was evaluated only with the proteins expressed differentially in the bands found; those with antioxidant function and those with interactions with statistical significance (PPI enrichment P-value ≤ 0.05) were included in the network analysis. When there were no reports on the European quail or the genus *Cortunix*, descriptions with the domestic rooster (*Gallus gallus*) were used.

2.4. Histology

Fragments of the testicles and epididymis were fixed by immersion in a 10% formaldehyde solution for 24 h. Subsequently, only the testes, being larger, were cut to obtain sizes close to 5 mm. Testicle and epididymis samples were placed in microtubes with fixation solution for technical processing, which consisted of the following steps: washing, dehydration, infiltration, and blocking. Samples were washed three times at 40-min intervals in 50% ethyl alcohol. After washing, the samples were dehydrated in an ethanol series at 50, 70, 90, and 100% ethanol, with 45 min between the different concentrations. The samples were infiltrated with historesin 1:1 ethyl alcohol for 48 h and again with historesin for 24 h. For blocking, the samples were placed in gelatin capsules, historesin and hardener were added and the capsules were exposed to light for 24 h. After historesin polymerization, the blocks were placed on pieces of wood, and cuts were made at 0.6 µm using a microtome (LEICA, Solms, Germany); the obtained slices were placed on slides for microscopy. Staining was performed with 1% toluidine blue solution, and the coverslips were placed with the aid of VERNIZ® (Acrilex). Images were captured using a Zeiss Primo Star microscope with an Axiocam 150 color capture camera, and the ZEN lite 2.1 software (Pleasanton, CA, USA) was used for image analysis. To collect image measurements, the Image J 1.8.0 software was used.

2.5. Statistical analysis

Statistical analysis was conducted considering a completely randomized design with four diets and six repetitions. Data were initially subjected to the Kolmogorov-Smirnov normality test to confirm normal distribution. When data were not normally distributed, they were log 10-transformed. Data were analyzed via one-way analysis of variance (ANOVA), according to the following general model:

$$Y_{ij} = \mu + \alpha_i + \varepsilon_{ij},$$

in which Y_{ij} is the measured dependent variable, μ is the overall mean, α_i is the treatment effect, and ε_{ij} is the random error.

Comparison among treatment averages was performed using Tukey's test at a significance level of 0.05. All analyses were performed using the R program (version 3.4.4).

3. Results

3.1. Testicular morphology

There was no significant (P≤0.05) effect of treatment on testicular weight, length, diameter, and volume as well as on the gonadosomatic index and weight of the birds (Table 2).

Table 2 - Testicular morphometric data and weights of European quail (*Coturnix coturnix coturnix*) fed different calcium anacardate levels (mean ± standard deviation)

	Calcium anacardate level (%)				P-value
	0 (control)	0.25	0.50	0.75	
Testicle weight (g)	3.83±1.24	3.91±0.29	4.91±0.77	3.94±1.22	0.283
Length (mm)	23.88±3.72	25.24±2.71	28.5±2.91	25.68±3.96	0.196
Diameter (mm)	16.86±1.97	17.66±0.90	19.6±1.56	17.46±1.97	0.132
Volume (cm^3)	3.68±1.39	4.12±0.50	5.82±1.34	4.22±1.65	0.075
TGI (%)	2.79±0.94	2.31±0.25	3.19±0.61	2.41±0.81	0.223
Final body weight (g)	295.9±8.4	327.25±17.2	309.49±16.1	328.24±17.1	0.063

TGI - testicular gonadosomatic index.

3.2. Proteomics data

Using 1-D electrophoresis, a total of 35 bands were observed in the testicular tissue gels of European quail, with molecular weights from 12 to 150 kDa (Figure 1). The intensity of 13 bands differed among treatments (Figure 2). Of the 13 bands, treatment with 0.75% CA was different from the control treatment in all bands. In two bands (29 and 32), with a molecular weight of 23 and 17 kDa, respectively, treatment with 0.75% CA differed from that with 0.25% CA.

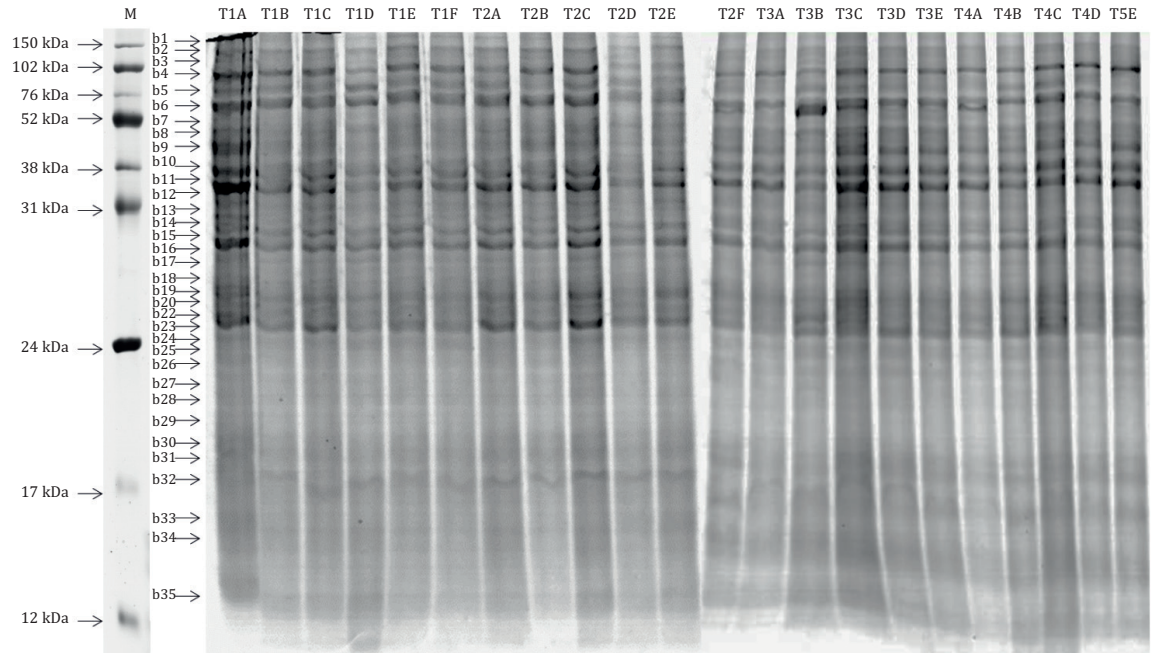

The experiment was divided into four treatments (1, 2, 3, and 4) and six repetitions (A, B, C, D, E, and F).
T1: control (0% calcium anacardate [CA]); T2: 0.25% CA; T3: 0.50% CA; T4: 0.75% CA.

Figure 1 - Protein polyacrylamide gel of European quail (*Coturnix coturnix coturnix*) testis with 12.5% SDS-PAGE stained with Coomassie blue.

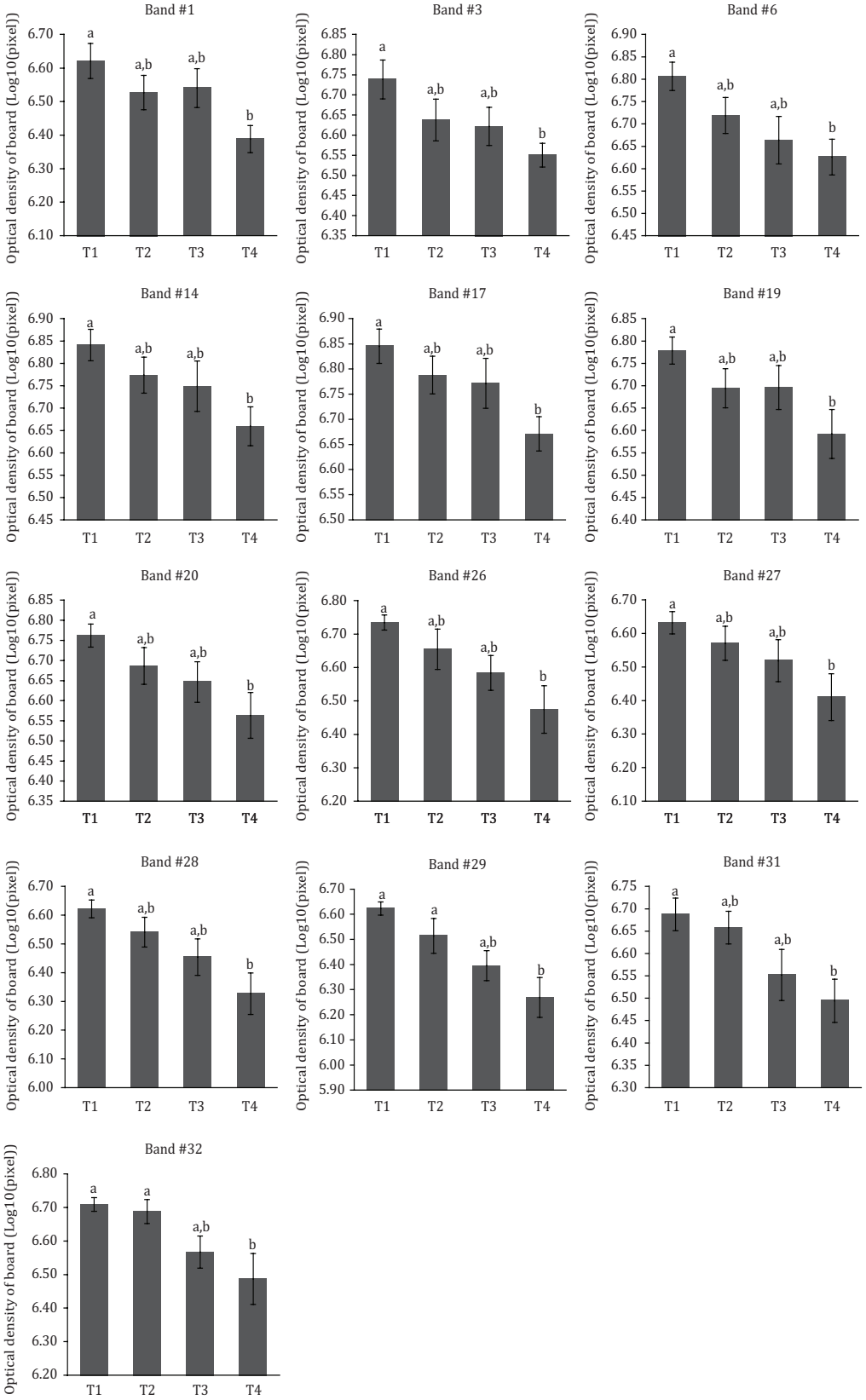

T1: control (0% calcium anacardate [CA]); T2: 0.25% CA; T3: 0.50% CA; T4: 0.75% CA.
Different letters indicate significantly different values (P<0.05).
Bars represent error bars.

Figure 2 - Profile of intensity of the testicular bands of European quail fed different calcium anacardate levels.

The 1-D electrophoresis and mass spectrometry allowed the identification of 152 proteins in the testes of European quail (Table 3), including heat shock cognate 71-kDa protein (HSPA8), stress-70 protein, mitochondrial (HSP9), superoxide dismutase [Cu-Zn] (SOD1), and peroxiredoxin-6 (PRDX6). Gene ontology was employed to collect data related to molecular function, biological processes, and cellular components of proteins found in the testes (Figure 3). In view of these results, the main functions of the proteins identified in the testicular tissue of European quail are binding (49%) and catalytic activity (36%), with only 1% being attributed to antioxidant activity.

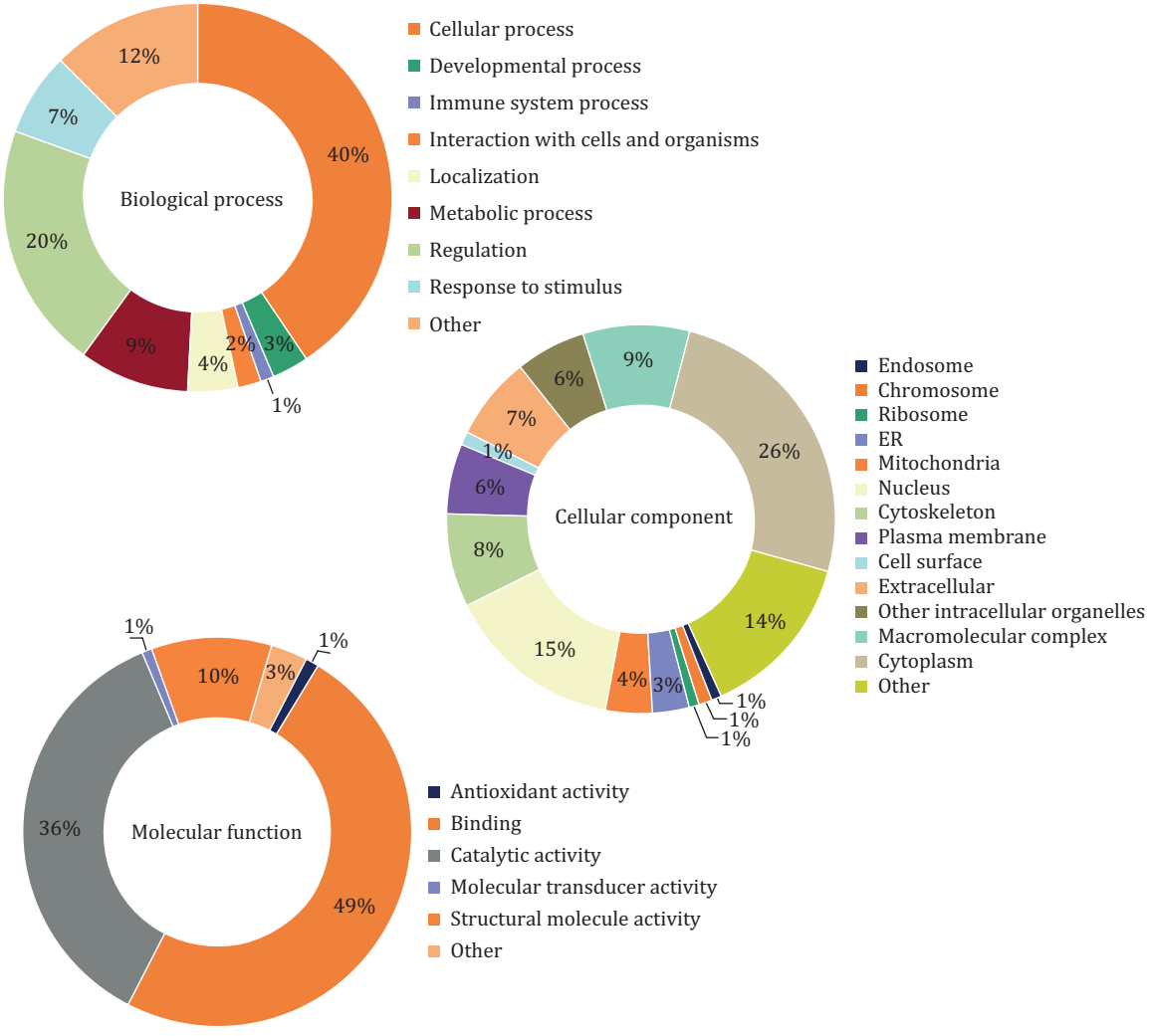

Source: STRAP.

Figure 3 - Gene ontology term annotations related to biological process, cellular component, and molecular function of the proteins from European quail testes.

Table 3 - Proteins[1] from the testicular tissue of European quail

Band	Protein	Gene name	Accession number		MS/MS protein score	Sequence covered (%)	Matched peptide	Ion score	m/z	z
1	PREDICTED: clathrin heavy chain 1 isoform X1	CLTC	XP_015735950.1	a	71	0	(1216)LLYNNVSNFGR(1226)	71	648.8392	2
2	PREDICTED: cullin-associated NEDD8-dissociated protein 1		XP_003202093.1	a	50	0	(607)AMTLIAGSPLK(617)	50	559.3221	2
	ubiquitin-like modifier-activating enzyme 1	ATG7	XP_024999761.1	a	33	4	(128)LAELNAYVGVSSSR(141)	33	473.4000	2
3	PREDICTED: ATP-citrate synthase isoform X1	ACLY	XP_015741119.1	a	175	2	(89)GQETTIANAK(99)	82	573.3089	2
							(663)SGGMSNELNNIISR(676)	93	754.3613	2
	PREDICTED: DNA damage-binding protein 1	DDB1	XP_015718677.1	a	72	0	(629)VTLGTQPTVLR(639)	74	592.8497	2
	PREDICTED: ubiquitin-like modifier-activating enzyme 1	ATG7	XP_015706618.1	a	75	7	(63)MQTSNVLVSGLR(74)	75	660.8475	2
4	PREDICTED: ubiquitin-like modifier-activating enzyme 1	N329_12388	XP_010571447.1	a	190	2	(68)MQTSNVLVSGLR(79)	98	660.8478	2
							(586)KPLLESGTLGTK(597)	91	622.3616	2
5	PREDICTED: alpha-actinin-1-like	ACTN1	XP_015720226.1	a	97	3	(174)TINEVENQILTR(185)	97	715.3821	2
	endoplasmin precursor	HSP90B1	NP_001310126.1	a	74	1	(75)FAFQAEVNR(83)	74	541.2708	2
	PREDICTED: heat shock 70 kDa protein 4L	HSPA8	XP_015716789.1	a	74	1	(111)LFAVEQITGMLLAK(124)	74	775.4452	2
	PREDICTED: heat shock protein HSP 90-beta	HSP90AB1	XP_005439121.1	a	72	1	(83)TLTLVDTGIGMTK(85)	75	675.3693	2
	PREDICTED: hexokinase-3 isoform X1	HK3	XP_015731713.1	a	253	3	(269)DVVQLLQAAISR(280)	82	658.8813	2
							(381)LVGSVYLGEIVR(392)	87	652.8768	2
							(982)GAALVAAVHSR(992)	85	525.7814	2
							(982)GAALVAAVHSR(992)	85	526.3007	2
	PREDICTED: puromycin-sensitive aminopeptidase	N/A	XP_015741316.1	a	89	1	(539)LGLQNDLFSLAR(550)	89	673.8649	2
	Transitional endoplasmic reticulum ATPase	AAES_64887	KQK82914.1	a	86	0	(1054)WALSQSNPSALR(1064)	86	665.3446	2
6	heat shock protein 75 kDa, mitochondrial	TRAP1	NP_001310167.1	a	114	1	(387)GVVDSEDIPLNLSR(400)	114	757.3970	2
							(387)GVVDSEDIPLNLSR(400)	96	757.3970	2
	heat shock protein HSP 90-alpha	HSP90AA1	NP_001310124.1	a	470	8	(209)HSQFIGYPIR(218)	82	609.3186	2
							(311)SLTNDWEDHLAVK(323)	112	764.3771	2
							(324)HFSVEGQLEFR(334)	76	674.8321	2
							(383)GVVDSEDLPLNISR(396)	114	757.3970	2
							(383)GVVDSEDLPLNISR(396)	96	757.3970	2
							(461)YYTSASGDEMVSLK(474)	94	783.8508	2
	piwi-like protein 1	PIWIL1	ADK95114.1	a	94	1	(507)NYDAANTLLQNLFK(520)	84	812.9166	2
	Transitional endoplasmic reticulum ATPase	AAES_64887	KQK82914.1	a	91	0	(878)LAGESESNLR(887)	91	538.2697	2

Continues...

Table 3 (Continued)

Band	Protein	Gene name	Accession number		MS/MS protein score	Sequence covered (%)	Matched peptide	Ion score	m/z	z
7	PREDICTED: heat shock protein 75 kDa, mitochondrial isoform X2	HSPA9	XP_015732760.1	a	100	1	(387)GVVDSEDIPLNLSR(400)	100	757.3993	2
	heat shock protein HSP 90-alpha	HSP90AA1	NP_001310124.1	a	187	5	(87)TLTIVDTGIGMTKADLVNNLGTIAK(111)	97	859.1378	3
							(383)GVVDSEDLPLNISR(396)	100	757.3993	2
8	PREDICTED: heat shock 70 kDa protein	HSPA8	XP_010150685.1	a	394	10	(5)GPAVGIDLGTTYSCVGVFQHGK(26)	85	755.0450	3
							(114)TFFPEEISSMVLTK(127)	75	822.9202	2
							(173)IINEPTAAAIAYGLDK(188)	71	830.4562	2
							(173)IINEPTAAAIAYGLDK(188)	81	830.4591	2
							(173)IINEPTAAAIAYGLDKK(188)	71	894.5104	2
							(332)GQIQEIVLVGGSTR(345)	81	728.9160	2
	heat shock cognate 71 kDa protein	HSPA8	NP_001310129.1	a	486	13	(4)GPAVGIDLGTTYSCVGVFQHGK(25)	85	755.0450	3
							(57)NQVAMNPTNTVFDAK(71)	86	833.4046	2
							(57)NQVAMNPTNTVFDAK(71)	72	833.4048	2
							(89)HWPFTVVNDAGRPK(102)	86	541.9496	3
							(138)TVTNAVVTVPAYFNDSQR(155)	76	991.5153	2
							(172)IINEPTAAAIAYGLDK(187)	71	830.4562	2
							(172)IINEPTAAAIAYGLDK(187)	81	830.4591	2
							(172)IINEPTAAAIAYGLDKK(188)	71	894.5104	2
	PREDICTED: serum albumin	ALB	XP_015717009.1	a	167	4	(48)AVAMITFAQYLQR(60)	72	764.4096	2
							(160)VSFLGHFIYSVAR(172)	99	748.4135	2
	PREDICTED: stress-70 protein, mitochondrial	HSPA9	XP_015731683.1	a	173	4	LYSPSQIGAFVLMK	91	785.4309	2
							LLGQFTLVGIPPAPR	82	789.9810	2
9	PREDICTED: bifunctional purine biosynthesis protein PURH	ATIC	XP_015723469.1	a	76	1	(125)IDIGGVALLR(134)	76	513.8188	2
	PREDICTED: eukaryotic translation initiation factor 3 subunit L, partial	EIF3D	XP_010154288.1	a	81	1	(121)VSGGPTLEQR(130)	83	522.2852	2
	PREDICTED: heat shock 70 kDa protein 4L isoform X3	N306_07292	XP_009944044.1	a	88	1	(129)VLATTFDPFIGGR(141)	88	697.3815	2
	heat shock protein 90kDa alpha (cytosolic), class A member 1	HSP90AA1	BAI23210.1	a	88	1	(461)YYTSASGDEMVSLK(474)	82	783.8612	2
	inducible heat shock protein 70	N/A	ACC85671.1	a	77	2	(38)TTPSYVAFTDTER(50)	77	744.3589	2
	PREDICTED: serum albumin	ALB	XP_015717009.1	a	79	2	(48)AVAMITFAQYLQR(60)	81	764.4085	2

Continues...

Table 3 (Continued)

Band	Protein	Gene name	Accession number		MS/MS protein score	Sequence covered (%)	Matched peptide	Ion score	m/z	z
10	heat shock protein 70kDa	HSPA2	BAF37039.1	a	81	2	(38)TTPSYVAFTDTER(50)	81	744.3629	2
	PREDICTED: pyruvate kinase PKM isoform X1	PKM	XP_015727855.1	a	405	11	(32)LDIDSEPTIAR(42)	77	615.3253	2
							(125)GSGTAEVELKK(135)	82	559.8095	2
							(230)FGVEQNVDMVFASFIR(245)	84	625.6403	2
							(383)EAEAAMFHR(391)	85	539.2463	2
							(406)EPADAMAAGAVEASFK(421)	78	790.8749	2
	PREDICTED: T-complex protein 1 subunit gamma	CCT3	XP_015739782.1	a	98	2	(439)AVAQALEVIPR(449)	98	583.8518	2
11	PREDICTED: glucose-6-phosphate isomerase	GPI	XP_015729552.1	a	154	5	(211)TFTTQETITNAVTAK(225)	82	813.4288	2
							(423)ILLANFLAQTEALMK(437)	74	846.4818	2
	PREDICTED: protein disulfide-isomerase A3	PDIA3	XP_015728935.1	a	166	5	(63)LAPEYEAAATR(73)	79	596.3029	2
							(131)QAGPASVALSSVADFEK(147)	87	838.9376	2
	PREDICTED: retinal dehydrogenase 1	ALDH1A1	XP_015704634.1	a	253	8	(109)LTLATMEAIDGGK(121)	79	668.3496	2
							(152)TVPMDGNFFTFTR(164)	76	774.8727	2
							(429)ANNTTYGLAAAVFTK(443)	98	771.4078	2
	PREDICTED: LOW QUALITY PROTEIN: T-complex protein 1 subunit alpha	CCT4	XP_015713526.1	a	88	2	(22)TQNVTAASAIANIVK(36)	88	750.9299	2
	PREDICTED: T-complex protein 1 subunit theta isoform X1	CCT8	XP_015736432.1	a	160	4	(282)AIADSGANVVVTGGK(296)	84	679.8680	2
							(441)FAEAFEAIPR(450)	76	575.7991	
12	PREDICTED: 60 kDa heat shock protein, mitochondrial	HSPD1	XP_015723158.1	a	77	3	(251)ISSVQSIVPALEIANSHR(268)	77	641.0191	3
	PREDICTED: retinal dehydrogenase 1	ALDH1A2	XP_015704634.1	a	93	2	(429)ANNTTYGLAAAVFTK(443)	93	771.4064	2
	ruvB-like 1	RCJMB04_28a17	NP_001006138.1	a	101	3	(318)ALESSISPIVIFASNR(333)	101	852.4755	2
	PREDICTED: T-complex protein 1 subunit theta isoform X1	CCT8	XP_015736432.1	a	92	2	(282)AIADSGANVVVTGGK(296)	92	679.8735	2
	PREDICTED: tubulin alpha-4A chain isoform X1		XP_015724463.1	a	77	2	(281)LIGQIVSSITASLR(294)	77	729.4388	2
	PREDICTED: tubulin alpha-8 chain	N/A	XP_015740341.1	a	77	3	(215)LIGQIVSSITASLR(228)	77	729.4388	2
	PREDICTED: tubulin beta chain	TUBB4B	XP_015706308.1	a	418	21	(6)SGPFGQIFRPDNFVFGQSGAGNNWAK(31)	75	933.4517	3
							(91)IMNTFSVVPSPK(102)	78	668.3556	2
							(145)LTTPTYGDLNHLVSATMSGVTTCLR(169)	87	908.7871	3
							(291)MSATFIGNSTAIQELFK(307)	87	937.4788	2
							(291)MSATFIGNSTAIQELFKR(308)	91	937.4788	3

Continues...

Table 3 (Continued)

Band	Protein	Gene name	Accession number		MS/MS protein score	Sequence covered (%)	Matched peptide	Ion score	m/z	z
13	PREDICTED: adenosylhomocysteinase	AHCYL1	XP_015736869.1	a	74	2	(176)VPAINVNDSVTK(187)	74	628.8489	2
	PREDICTED: alpha-enolase isoform X1	ENO1	XP_015738218.1	a	383	13	(16)GNPTVEVDVYTNK(28)	78	718.3589	2
							(163)LAMQEFMILPVGASSFK(179)	92	950.9882	2
							(240)VVIGMDVAASEFYR(253)	110	786.8961	2
							(344)VNQIGSVTESLQACK(358)	102	817.4188	2
	eukaryotic initiation factor 4A-II	EIF4A2	NP_989880.1	a	150	7	(70)GYDVIAQAQSGTGK(83)	76	697.8532	2
							(148)LQAEAPHIVVGTPGR(162)	74	772.9360	2
	PREDICTED: tubulin beta chain	TUBB4B	XP_015706308.1	a	334	17	(91)IMNTFSVVPSPK(102)	81	668.3563	2
							(145)LTTPTYGDLNHLVSATMSGVTTCLR (169)	96	908.7867	3
							(181)LAVNMVPFPR(191)	78	580.3173	2
							(291)MSATFIGNSTAIQELFK(307)	79	937.4789	2
	PREDICTED: tubulin beta-3 chain	N/A	XP_015729712.1	a	332	7	(583)IMNTFSVVPSPK(594)	81	668.3563	2
							(637)LTTPTYGDLNHLVSATMSGVTTCLR (661)	96	908.7867	3
							(673)LAVNMVPFPR(682)	78	580.3173	2
							(783)MSATFIGNSTAIQELFK(789)	79	937.4789	2
14	PREDICTED: actin, cytoplasmic 1	KDR	XP_015732105.1	a	75	2	(29)AVFPSIVGRPR(39)	77	599.8603	2
	LOW QUALITY PROTEIN: alpha-centractin	AAES_129494	XP_023785541.1	a	171	8	(47)VMAGALEGDIFIGPK(61)	84	767.4163	2
							(293)TLFSNIVLSGGSTLFK(308)	87	842.4752	2
	beta-actin, partial	N/A	AAF13710.1	a	75	3	(8)AVFPSIVGRPR(18)	77	599.8603	2
	PREDICTED: long-chain specific acyl-CoA dehydrogenase, mitochondrial		XP_015723434.1	a	78	3	(78)AGQQGLLGVAIAEK(107)	78	677.8937	2
	PREDICTED: tubulin alpha-3 chain	N/A	XP_015727678.1	a	167	6	(216)NLDIERPTYTNLNR(229)	85	573.6298	3
							(230)LIGQIVSSITASLR(243)	83	729.4414	2
15	PREDICTED: 40S ribosomal protein SA	RPSA	XP_009999990.1	a	266	15	(64)AIVAIENPADVSVISSR(80)	77	870.9827	2
							(90)FAAATGATPIAGR(102)	88	602.3286	2
							(103)FTPGTFTNQIQAAFR(117)	101	849.9354	2
	PREDICTED: alpha-enolase isoform X1	ENO1	XP_015738218.1	a	74	3	(240)VVIGMDVAASEFYR(253)	74	786.8980	2
	PREDICTED: aspartate aminotransferase, mitochondrial	GOT2	XP_015729073.1	a	87	3	(119)YVTVQGISGTGSLR(132)	89	719.3927	2
	PREDICTED: enoyl-CoA delta isomerase 2, mitochondrial isoform X1		XP_015710037.1	a	100	3	(118)LVSSLVSAESAVQK(131)	100	709.3995	2

Continues...

Table 3 (Continued)

Band	Protein	Gene name	Accession number		MS/MS protein score	Sequence covered (%)	Matched peptide	Ion score	m/z	z
	PREDICTED: gamma-enolase isoform X2	ENO2	XP_015728224.1	a	74	3	(240)VVIGMDVAASEFYR(253)	74	786.8980	2
	PREDICTED: tubulin alpha-1C chain		XP_015742375.1	a	93	3	(216)NLDIERPTYTNLNR(229)	93	573.6297	3
16	PREDICTED: desmin	DES	XP_015724646.1	a	78	2	(388)LALDIEIATYR(398)	78	639.3552	2
	PREDICTED: leucine zipper transcription factor-like protein 1	N/A	XP_015709640.1	a	164	9	(138)LAPINEGESELLNK(151)	86	763.9097	2
							(169)TIETQATAALDEK(181)	77	695.8533	2
	PREDICTED: protein phosphatase 1 regulatory subunit 7 isoform X1	PPP1R7	XP_015726561.1	a	89	2	(340)IEGLQSLVNLR(350)	89	621.3622	2
17	Glyceraldehyde-3-phosphate dehydrogenase	GAPDH	G3P_COTJA	a	307	15	(65)LVINGNAITIFQER(78)	80	794.4468	2
							(65)LVINGNAITIFQER(78)	80	794.9444	2
							(161)VIHDNFGIVEGLMTTVHAITATQK(184)	78	653.5869	4
							(161)VIHDNFGIVEGLMTTVHAITATQK(184)	120	871.1222	3
							(161)VIHDNFGIVEGLMTTVHAITATQK(184)	111	871.1224	3
							(233)VPTPNVSVVDLTCR(246)	106	778.9113	2
							(233)VPTPNVSVVDLTCR(246)	108	778.9136	2
	PREDICTED: leucine zipper transcription factor-like protein 1	N/A	XP_015709640.1	a	247	11	(128)KPNAELIKPK(137)	70	379.8971	2
							(138)LAPINEGESELLNK(152)	94	763.9112	2
							(262)KFQQTAAYR(270)	83	556.7965	2
	PREDICTED: malate dehydrogenase, cytoplasmic	MDH1	XP_015712071.1	a	154	9	(48)VLVTGAAGQIAYSLLYSIAK(67)	76	1019.5819	2
							(167)VVVVGNPANTNCLIASK(183)	79	878.4799	2
	PREDICTED: protein disulfide-isomerase A6	AAES_129824	XP_015714908.1	a	82	3	(223)LAAVDATVNQMLASR(237)	82	780.4155	2
							(223)LAAVDATVNQMLASR(237)	78	788.4127	2
18	PREDICTED: 60S acidic ribosomal protein P0	RPLP0	XP_015733447.1	a	86	9	(267)AFLADPSAFVAAAPVVTETAA PAAAAAPAK (296)	86	923.1642	3
	PREDICTED: LOW QUALITY PROTEIN: aldose reductase-related protein 1-like	AV530_009719	XP_015720325.1	a	122	22	(23)SPPGQVTAAVMAAIDAGYR(41)	73	630.9796	2
							(23)SPPGQVTAAVMAAIDAGYR(41)	122	945.9779	2
	PREDICTED: F-actin-capping protein subunit alpha-2	CAPZA2	XP_015709129.1	a	156	7	(65)LLLNNDNLLR(74)	77	599.3503	2
							(206)FTISPSTTQVAGILK(220)	79	781.9471	2

Continues...

Table 3 (Continued)

Band	Protein	Gene name	Accession number		MS/MS protein score	Sequence covered (%)	Matched peptide	Ion score	m/z	z
	Glyceraldehyde-3-phosphate dehydrogenase	GAPDH	G3P_COTJA	a	163	11	(161)VIHDNFGIVEGLMTTVHAITATQK(184)	83	653.5871	4
							(161)VIHDNFGIVEGLMTTVHAITATQK(184)	83	871.1256	3
							(233)VPTPNVSVVDLTCR(246)	80	778.9072	2
	PREDICTED: glyoxylate reductase/hydroxypyruvate reductase	CTBP2	XP_015705574.1	a	81	4	(301)STMAVLAADNLLAGLR(316)	81	816.4471	2
	PREDICTED: leucine zipper transcription factor-like protein 1	N/A	XP_015709640.1	a	72	4	(169)TIETQATAALDEK(181)	72	695.8591	2
	PREDICTED: malate dehydrogenase, cytoplasmic	MDH1	XP_015712071.1	a	318	18	(48)VLVTGAAGQIAYSLLYSIAK(67)	76	1019.5865	2
							(108)EVIPTDKEEVAFK(120)	73	752.9024	2
							(167)VVVVGNPANTNCLIASK(183)	93	878.4757	2
							(221)NVIIWGNHSSTQYPDVNHAK(240)	76	760.7101	3
	PREDICTED: nascent polypeptide-associated complex subunit alpha	AAES_69056	XP_015742550.1	a	186	9	(101)NILFVITKPDVYK(113)	74	775.4572	2
							(114)SPASDTYIVFGEAK(127)	112	742.8696	2
	PREDICTED: nuclease-sensitive element-binding protein 1 isoform X1	YBX1	XP_015737879.1	a	74	5	(117)GAEAANVTGPGGVPVQGSK(135)	74	848.4360	2
	PREDICTED: ribose-phosphate pyrophosphokinase 1 isoform X2	PRPS2	XP_015715595.1	a	73	6	(186)VYAILTHGIFSGPAISR(202)	73	601.3344	3
19	elongation factor 1-alpha, partial	EF1A	AJP09268.1	a	75	4	(110)IGGIGTVPVGR(120)	75	513.3057	2
	PREDICTED: hydroxyacyl-coenzyme A dehydrogenase	AAES_156447	XP_015716844.1	a	78	8	(138)FAPEHTIFASNTSSLQITQLANSTTR(163)	78	945.8050	3
	PREDICTED: L-lactate dehydrogenase B chain	LDHB	XP_015724692.1	a	271	11	(119)LKGEMMDLQHGSLFLQTHK(137)	72	749.0367	3
							(138)IVADKDYAVTANSK(151)	113	747.8944	2
							(219)VIGSGCNLDSAR(230)	86	624.8006	2
	PREDICTED: malate dehydrogenase, mitochondrial	MDH1	XP_015736217.1	a	255	16	(26)VAVLGASGGIGQPLSLLLK(44)	91	897.0472	2
							(52)LTLYDIAHTPGVAADLSHIETR(73)	79	599.0584	4
							(52)LTLYDIAHTPGVAADLSHIETR(73)	77	798.4217	4
							(241)AGAGSATLSMAYAGAR(256)	85	735.8523	2
	PREDICTED: ribose-phosphate pyrophosphokinase 1 isoform X2	PRPS2	XP_015715595.1	a	86	6	(186)VYAILTHGIFSGPAISR(202)	86	601.3322	3
	PREDICTED: S-formylglutathione hydrolase isoform X1	ESD	XP_015707271.1	a	82	4	(131)LINANFPTNPER(142)	82	693.3601	2
	PREDICTED: tubulin beta chain	TUBB4B	XP_015706308.1	a	82	2	(181)LAVNMVPFPR(190)	82	580.3172	2
	PREDICTED: UPF0769 protein C21orf59 homolog		XP_003202943.1	a	78	3	(24)LAELAPLVAR(33)	78	526.8258	2

Continues...

Table 3 (Continued)

Band	Protein	Gene name	Accession number		MS/MS protein score	Sequence covered (%)	Matched peptide	Ion score	m/z	z
20	PREDICTED: L-lactate dehydrogenase B chain	LDHB	XP_015724692.1	a	81	3	(219)VIGSGCNLDSAR(230)	81	624.8006	2
	PREDICTED: T-complex protein 1 subunit gamma	CCT3	XP_015739782.1	a	78	2	(439)AVAQALEVIPR(449)	78	583.8463	2
	PREDICTED: T-complex protein 1 subunit theta isoform X1	CCT8	XP_015736432.1	a	179	4	(282)AIADSGANVVVTGGK(296)	96	679.8655	2
							(510)LATNAAVTVLR(520)	83	564.8373	2
	PREDICTED: tubulin alpha-8 chain	N/A	XP_015740341.1	a	71	3	(215)LIGQIVSSITASLR(228)	71	729.4359	2
21	PREDICTED: proteasome assembly chaperone 1 isoform X1	PSMG1	XP_015738121.1	a	89	4	(171)TQESTLTLPSPFLK(184)	89	781.4274	2
	PREDICTED: T-complex protein 1 subunit gamma	CCT3	XP_015739782.1	a	154	4	(439)AVAQALEVIPR(449)	78	583.8492	2
							(508)TAVETAVLLLR(518)	78	593.3637	2
	PREDICTED: T-complex protein 1 subunit theta isoform X1	CCT8	XP_015736432.1	a	259	6	(282)AIADSGANVVVTGGK(296)	89	679.8650	2
							(441)FAEAFEAIPR(450)	89	575.7988	2
							(510)LATNAAVTVLR(520)	81	564.8379	2
	PREDICTED: tubulin alpha-3 chain	N/A	XP_015727678.1	a	74	3	(230)LIGQIVSSITASLR(243)	73	729.4351	2
							(230)LIGQIVSSITASLR(243)	74	729.4359	2
	UPF0769 protein C21orf59 homolog	C1H21ORF59	NP_001006258.1	a	71	3	(24)LAELAPLVAR(33)	71	526.8272	2
	PREDICTED: voltage-dependent anion-selective channel protein 2 isoform X2	AAES_208041	XP_015722112.1	a	84	7	(237)VNNSSLVGLGYTQTLRPGVK(256)	84	701.7223	3
22	Proteasome subunit alpha type-3, partial	Z169_11543	KFP16057.1	a	77	5	(23)AVENSSTAIGIR(34)	77	603.3268	2
	PREDICTED: tubulin beta-1 chain isoform X2	N/A	XP_015737231.1	a	91	3	(91)IMNTFSVVPSPK(102)	81	668.3499	2
23	PREDICTED: 60S ribosomal protein L7	RPL7	XP_015711270.1	a	98	4	(165)IALTDNSLIR(174)	98	558.3220	2
							(165)IALTDNSLIR(174)	77	558.3220	2
	PREDICTED: heterogeneous nuclear ribonucleoprotein H isoform X7	HNRNPH2	XP_015731198.1	a	73	1	(66)ILNGPLGIR(74)	73	476.7979	2
	PREDICTED: keratin, type II cytoskeletal 5-like		XP_015742493.1	a	73	1	(214)SLNNKFASFIDK(225)	73	692.3505	2
	PREDICTED: phosphoglycerate mutase 1	PGAM1	XP_015722493.1	a	161	10	(215)VLIAAHGNSLR(225)	77	575.8371	2
							(257)NLKPVKPMQFLGDAETVR(274)	84	687.0345	4
	PREDICTED: proteasome subunit beta type-3	PSMB3	XP_015741214.1	a	91	8	(49)LYIGLAGLATDVQTVAQR(66)	91	945.0304	2
	PREDICTED: T-complex protein 1 subunit beta	CCT5	XP_015711605.1	a	187	5	(389)SLHDALCVLAQTVK(402)	104	777.9193	2
							(502)QVLLSAAEAAEMILR(516)	84	815.9497	2

Continues...

Table 3 (Continued)

Band	Protein	Gene name	Accession number		MS/MS protein score	Sequence covered (%)	Matched peptide	Ion score	m/z	z
	PREDICTED: T-complex protein 1 subunit gamma	CCT3	XP_015739782.1	a	99	2	(439)AVAQALEVIPR(449)	99	583.8474	2
	PREDICTED: tubulin alpha-3 chain	N/A	XP_015727678.1	a	76	3	(230)LIGQIVSSITASLR(243)	76	729.4392	2
24	elongation factor 1-alpha, partial	EF1A	AJP09268.1	a	73	4	(110)IGGIGTVPVGR(120)	73	513.3056	2
	PREDICTED: leucine zipper transcription factor-like protein 1	N/A	XP_015709640.1	a	82	3	(98)LQTDISELENR(108)	82	659.3367	2
	PREDICTED: phosphoglycerate mutase 1	PGAM1	XP_015722493.1	a	226	16	(100)TLWNVLDAIDQMWLPVVR(117)	72	1093.0885	2
							(215)VLIAAHGNSLR(225)	72	384.2213	3
							(257)NLKPVKPMQFLGDAETVR(274)	82	687.0359	3
	PREDICTED: proline synthase co-transcribed bacterial homolog protein	PROSC	XP_015738610.1	a	73	4	(192)GPNPDFQVLLSLR(204)	73	728.4049	2
	PREDICTED: tubulin alpha-3 chain	N/A	XP_015727678.1	a	74	3	(230)LIGQIVSSITASLR(243)	74	729.4400	2
25	PREDICTED: 60S ribosomal protein L10a		XP_015740653.1	a	73	5	(106)KYDAFLASESLIK(118)	73	742.9061	2
	PREDICTED: 6-phosphogluconolactonase	PGLS	XP_015705947.1	a	77	6	(33)FTLGLSGGSLVGLLAR(48)	77	780.9636	2
	Apolipoprotein A-I	APOA1	APOA1_COTJA	b	73	3	(219)VVEQLSNLR(227)	73	529.3008	2
	PREDICTED: C-factor-like		XP_015729251.1	a	91	5	(152)AAIINISTVLGSIER(166)	91	778.9551	2
	elongation factor 1-alpha, partial	EF1A	AJP09268.1	a	77	4	(110)IGGIGTVPVGR(120)	77	513.3095	2
	PREDICTED: peroxiredoxin-6	PRDX6	XP_015724871.1	a	163	12	(24)FHDFLGDSWGILFSHPR(40)	75	677.6623	3
							(162)VVDSLQLTAYK(172)	88	618.8439	2
	PREDICTED: protein SGT1 homolog		XP_015707211.1	a	82	4	(64)SLELNPSNAIALLR(77)	82	755.9357	2
	PREDICTED: protein syndesmos	NUDT16L1	XP_015732887.1	a	76	5	(182)MGGLPNFLANSFVGPAK(198)	76	868.4495	2
	PREDICTED: pseudouridine-5'-phosphatase isoform X1		XP_015704461.1	a	73	3	(61)ALEGAQIVR(69)	75	478.7775	2
	PREDICTED: triosephosphate isomerase	TPI1	XP_015728262.1	a	147	10	(160)VVLAYEPVWAIGTGK(174)	74	801.9460	2
							(194)SHVSDAVAQSTR(205)	73	629.3153	2
	PREDICTED: tubulin alpha-8 chain	N/A	XP_015740341.1	a	74	3	(215)LIGQIVSSITASLR(228)	74	729.4400	2
	PREDICTED: UPF0568 protein C14orf166 homolog		XP_015721446.1	a	97	5	(132)AGVMALANLLQIQR(145)	97	757.4320	2
26	PREDICTED: triosephosphate isomerase	TPI1	XP_015728262.1	a	172	11	(160)VVLAYEPVWAIGTGK(174)	78	801.9532	2
							(206)IIYGGSVTGGNCK(218)	94	663.3273	2
	PREDICTED: tubulin beta chain	TUBB4B	XP_015706308.1	a	98	2	(170)FPGQLNADLR(179)	98	565.8027	2
27	PREDICTED: aflatoxin B1 aldehyde reductase member 2		XP_015737793.1	a	74	4	(189)FYAYNPLAGGLLTGK(203)	74	792.9374	2
	Apolipoprotein A-I	APOA1	APOA1_COTJA	b	97	5	(69)LADNLDTLSAAAAK(82)	97	687.3734	2

Continues...

Table 3 (Continued)

Band	Protein	Gene name	Accession number		MS/MS protein score	Sequence covered (%)	Matched peptide	Ion score	m/z	z
	PREDICTED: creatine kinase B-type isoform X2	CKB	XP_015720975.1	a	76	3	(152)LSVEALGSLSGDLK(165)	76	694.8885	2
	Glyceraldehyde-3-phosphate dehydrogenase	GAPDH	G3P_COTJA	b	72	7	(161)VIHDNFGIVEGLMTTVHAITATQK(184)	72	653.5927	5
28	Glyceraldehyde-3-phosphate dehydrogenase	GAPDH	G3P_COTJA	b	155	11	(65)LVINGNAITIFQER(78)	72	794.4517	2
							(161)VIHDNFGIVEGLMTTVHAITATQK(184)	82	871.1240	3
	PREDICTED: tubulin alpha-3 chain	N/A	XP_015727678.1	a	78	3	(230)LIGQIVSSITASLR(243)	78	729.4408	2
	PREDICTED: tubulin beta chain	TUBB4B	XP_015706308.1	a	74	3	(91)IMNTFSVVPSPK(102)	74	668.3594	2
29	PREDICTED: adenylate kinase isoenzyme 1 isoform X2	AK1	XP_015734868.1	a	74	7	(110)IGPPTLLLYVDAGK(123)	74	728.9299	2
	Glyceraldehyde-3-phosphate dehydrogenase	GAPDH	G3P_COTJA	b	185	11	(65)LVINGNAITIFQER(78)	93	794.4517	2
							(65)LVINGNAITIFQER(78)	100	794.4542	2
							(161)VIHDNFGIVEGLMTTVHAITATQK(184)	84	871.1 240	3
	PREDICTED: tubulin beta-1 chain isoform X2	N/A	XP_015737231.1	a	71	3	(91)IMNTFSVVPSPK(102)	71	668.3535	2
30	heat shock protein 90 alpha, partia	N/A	AAL83217.1	a	73	5	(87)TLTIVDTGIGMTK(99)	73	683.3676	2
31	PREDICTED: tumor protein D54 isoform X1	AAES_188100	XP_015737294.1	a	94	5	(163)TSAALSNVGSVISR(176)	94	681.3772	2
32	PREDICTED: LOW QUALITY PROTEIN: proteasome subunit beta type-5	PSMB5	XP_015706419.1	a	91	5	(73)ATAGSYIASQTVQK(86)	91	712.8786	2
33	PREDICTED: heat shock protein HSP 90-beta	HSP90AB1	XP_005238716.1	a	76	1	(83)TLTLVDTGIGMTK(95)	78	683.3657	2
	PREDICTED: tubulin beta chain	TUBB4B	XP_015706308.1	a	85	4	(291)MSATFIGNSTAIQELFK(307)	85	937.4821	2
34	O-acetyl-ADP-ribose deacetylase 1	AAES_32060	KQL52048.1	a	76	5	(84)TGEVAVLQR(92)	76	486.7772	2
	PREDICTED: prefoldin subunit 5	VBP1	XP_015705869.1	a	74	10	(139)IQQLTAMGAAQGATTK(154)	74	803.4242	2
	PREDICTED: superoxide dismutase [Cu-Zn]	SOD1	XP_015736733.1	a	75	12	(12)GDGPVEGVIHFQQQGSGPVK(31)	75	679.3410	4
35	Glyceraldehyde-3-phosphate dehydrogenase	GAPDH	G3P_COTJA	b	92	4	(233)VPTPNVSVVDLTCR(246)	92	778.9147	2
	PREDICTED: profilin-1-like		XP_015130231.1	a	75	7	(27)DTPAVWAATPGK(38)	75	607.3161	2
	PREDICTED: protein disulfide-isomerase A6	AAES_129824	XP_015714908.1	a	76	3		76	708.8924	2

[1] The proteins were separated by one-dimensional electrophoresis (SDS-page) and identified by mass spectrometry (ESI-Q-TOF) identification of the proteins expressed in the testicular tissue of European quail fed different calcium anacardate levels.
a: NCBI; b: SwissProt.
MS/MS - mass spectrometry; m/z - mass-to-charge ratio; z - number of ions.

Protein interactions for five proteins involved in antioxidative processes and that differed significantly among treatments from each other in this study (P≤0.05) were analyzed. The proteins were superoxide dismutase [Cu-Zn] (SOD1), peroxideroxin-6 (PRDX6), stress-70 protein (HSPA9), 60-kDa heat shock protein (HSPD1), and heat shock cognate 71-kDa protein (HSPA8). Figure 4 illustrates the interaction of these five proteins, and Figure 5 illustrates the interactions of each mentioned protein with other proteins. Peroxiredoxin-6 showed co-expression interaction with proteins that protect the body against oxidative agents, such as catalase and superoxide dismutase [Cu-Zn] SOD1 (Figure 5A). Superoxide dismutase [Cu-Zn] showed a text-mining interaction with other proteins capable of extinguishing radicals produced during oxidative stress, such as catalase and thioredoxin (Figure 5B). The HSPD1 protein was also found in this study. This protein, which is considered an HSP60, has co-expression and text-mining with HSP70, and therefore, both have similar biochemical characteristics (Becker and Craig, 1994) (Figure 5C). The HSPA9 protein showed a text-mining interaction with proteins responsible for protecting other proteins from oxidative stress (60-kDa heat shock protein, mitochondrial, and DnaJ homolog subfamily B member 6; Figure 5D).The HSPA8 protein was also found in this study, with co-expression interproteic interaction with HSP70 and DJ-1 protein (Figure 5E).

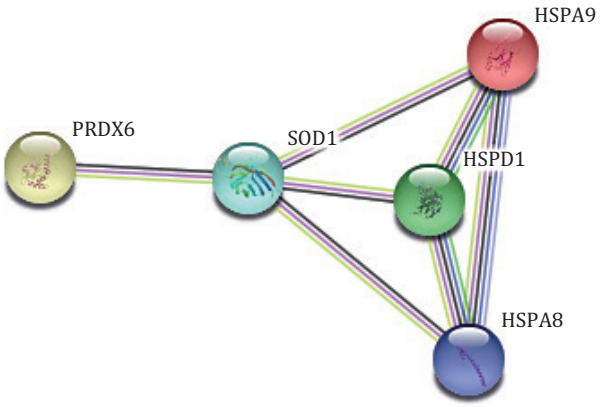

SOD1 - superoxide dismutase [Cu - Zu]; PRDX6 - peroxideroxin-6; HSPA9 - stress-70 protein; HSPD1 - 60-kDa heat shock protein; HSPA8 - heat shock cognate 71-kDa protein.
Different colored lines represent the types of evidence for the association: (–) text-mining; (–) experiments; (–) co-expression; (–) co-occurrence; (–) neighborhood gene; (–) homology.
Source: STRING.

Figure 4 - Interprotein-protein interaction networks obtained through the STRING application, showing interactions in evidence mode.

3.3. Histology characteristics

The diameter of the seminiferous tubules of quail was not influenced by treatments. However, the height of the seminiferous epithelium and the diameter of the epididymal duct significantly differed among treatments (Table 4). There was no significant effect of treatments on the quantities of testicle cells of quail (Table 5). Through optical microscopy, images of the seminiferous tubule (Figure 6) and the epididymis (Figure 7) of European quail were captured, with germ cells at different stages of development, as well as Sertoli and Leydig cells (Figures 6 and 7) and sperm formed in the epididymis. Hair and non-hair cells in the efferent duct could also be observed.

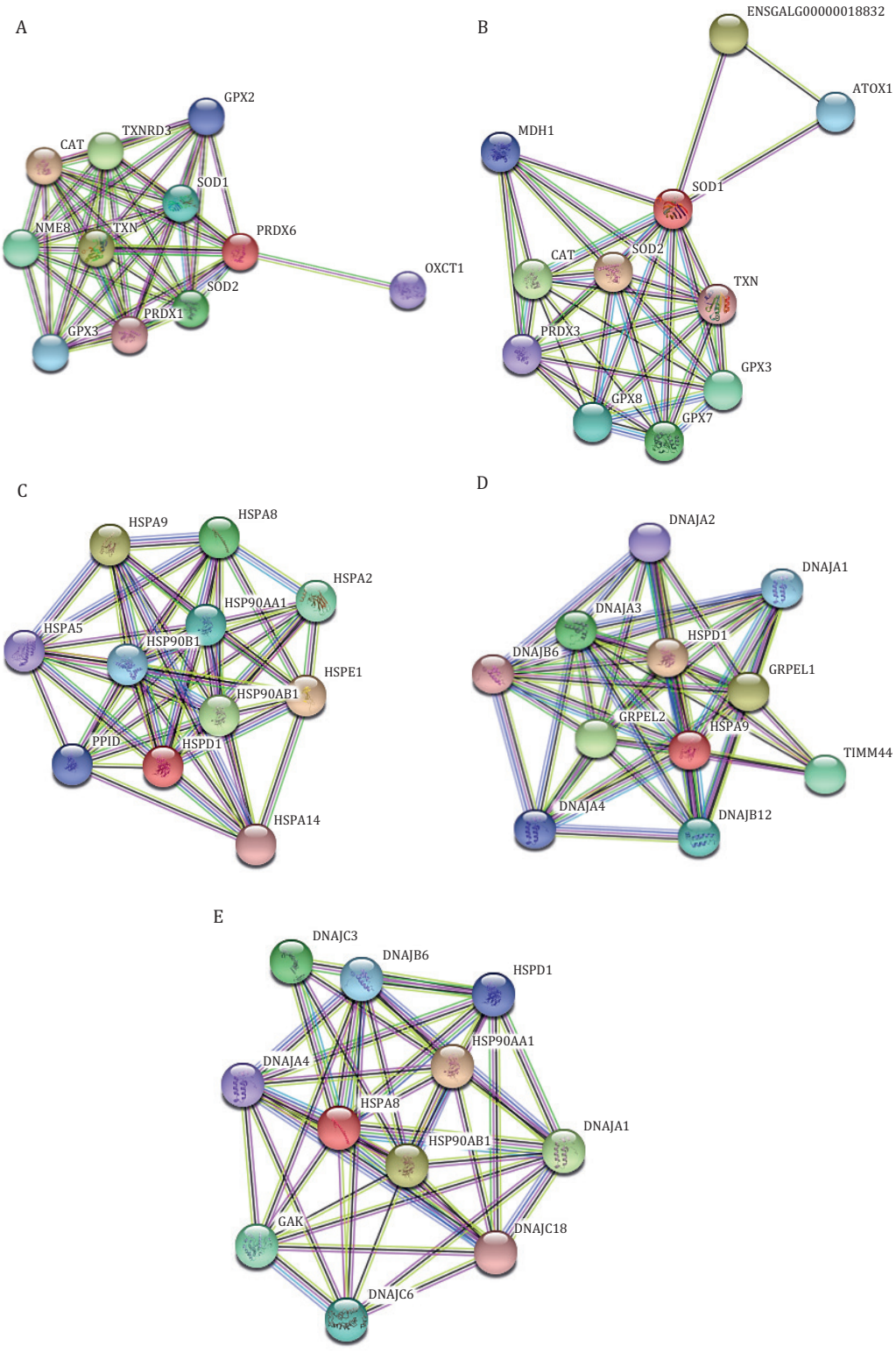

A: peroxiredoxin-6 (PRDX6); B: superoxide dismutase [Cu-Zu] (SOD1); C: 60-kDa heat shock protein, mitochondrial (HSPD1); D: stress-70 protein, mitochondrial (HSPA9); E: heat shock cognate 71-kDa protein (HSPA8).
Different colored lines represent the types of evidence for the association: (–) text-mining; (–) experiments; (–) co-expression; (–) co-occurrence; (–) neighborhood gene; (–) homology.
Source: STRING.

Figure 5 - *In silico* analysis of the interproteic interaction networks of proteins that were differentially expressed in the testes of European quail (*Coturnix coturnix coturnix*), obtained based on the STRING database to verify interactions with other proteins that have antioxidant function.

Table 4 - Mean testicular and epididymis morphological parameters of European quail fed different calcium anacardate levels (mean ± standard deviation)

Parameter	Calcium anacardate level (%)				P-value
	0 (control)	0.25	0.50	0.75	
STD (µm)	183.5±7.9	202.8±23.4	185.8±19.2	221.3±38.3	0.095
HSE (µm)	71.2±17.5a	70.1±19.8a	41.2±11.3b	45.6±14.8b	0.00068
EDD (µm)	29.9±13.4b	50.1±29.5b	46.2±20.2b	101.5±65.8a	0.0000017

STD - seminiferous tubule diameter; HSE - height of the seminiferous epithelium; EDD - epididymal duct diameter.
Means followed by the same letter within a row do not differ significantly from each other by Tukey's test at 5% probability.

Table 5 - Number of cells present in the seminiferous tubules of testes from European quail fed different calcium anacardate levels (mean ± standard deviation)

Cell	Calcium anacardate level (%)				P-value
	0 (control)	0.25	0.50	0.75	
Spermatogonia	38±4.24	58±19.78	71.5±14.84	73.5±24.74	0.853
Spermatocytes	104.5±20.5	86±12.7	146±19.7	120.5±9.19	0.121
Spermatids	228.5±26.1	309.5±27.6	329±26.9	287±38.9	0.336

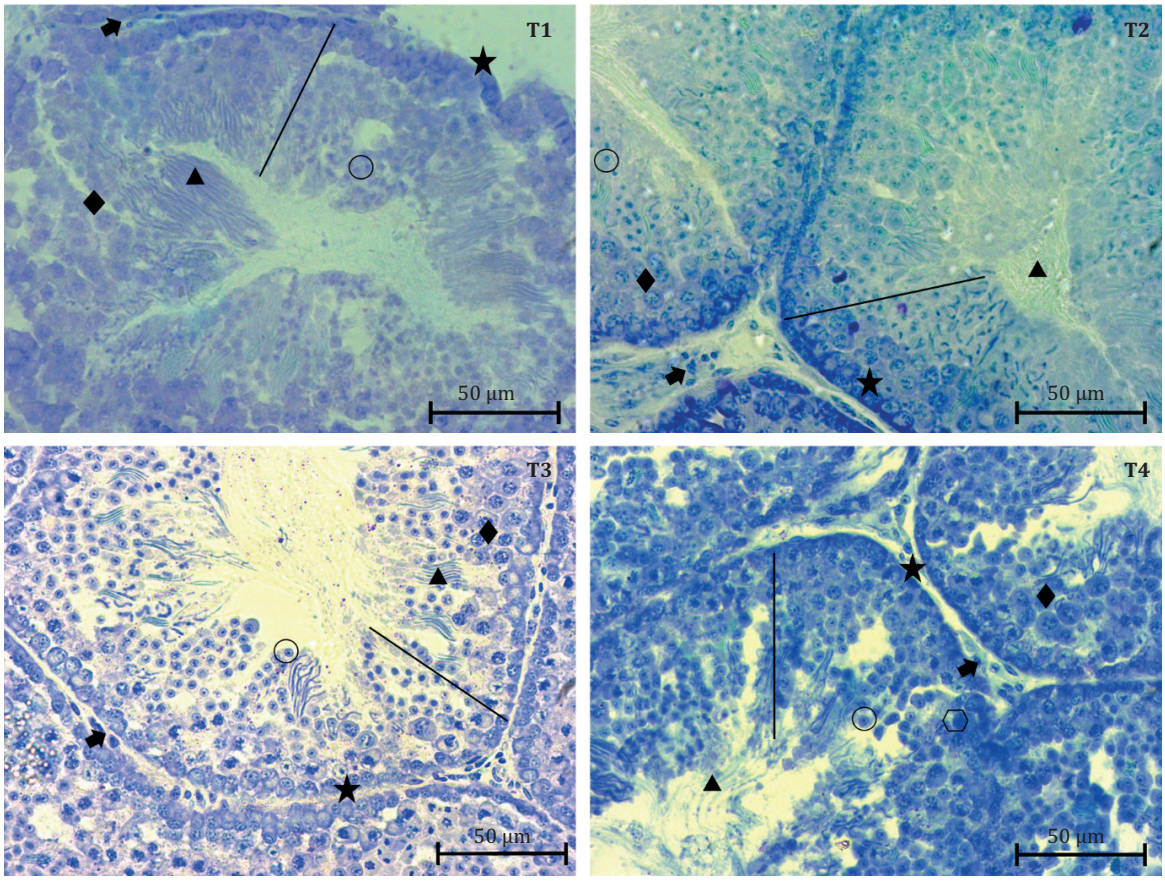

Spermatogonia (★); spermatocytes (◆); spermatids (○); sperm (▲); Leydig cell (⬇); Sertoli cell (⬡); seminiferous epithelium (–).
Source: ZEN Lite 2.1.

Figure 6 - Light microscopy images of the seminiferous tubule of European quail of 210 days of age fed different calcium anacardate levels during 70 days.

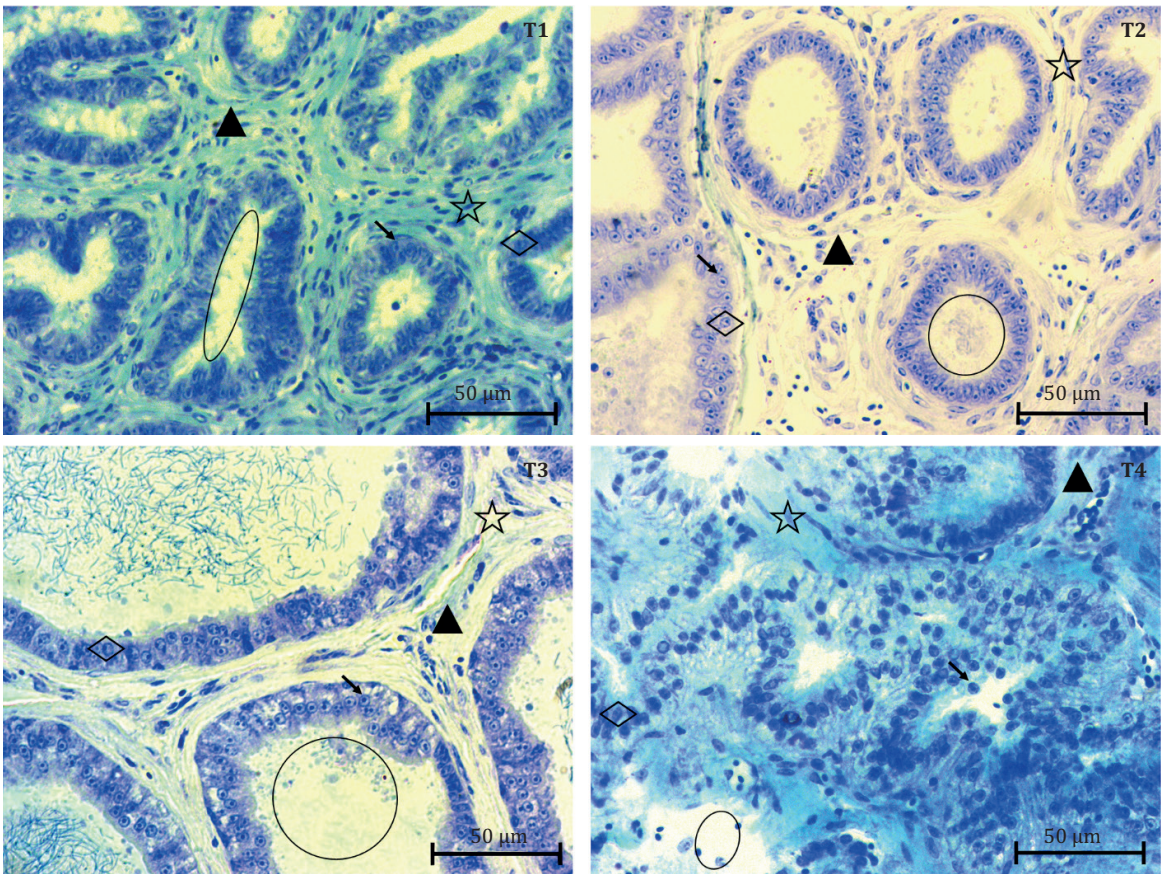

Efferent duct (◯); epididymal duct (▲); sperm (☆); unciliated main cell (◇); main hair cell (➞).
Source: ZEN lite 2.1.

Figure 7 - Light microscopy images of the epididymis of European quail of 210 days of age fed different calcium anacardate levels during 70 days.

4. Discussion

4.1. Testicular morphology

The reproductive system of birds differs from that of mammals in that it does not have important glands for semen production, such as the bulbourethral gland, the seminal vesicle, and the prostate. In addition, the epididymis of birds does not have a head, body, and tail division such as the epididymis of mammals (Macari and Maiorka, 2017). Animals subjected to a high-temperature environments undergo heat stress, inducing the production of ROS, which in turn induces molecular, physiological, and morphological changes in the reproductive organs, affecting reproduction (Hanafi et al., 2010). Garrigue et al. (2017), when subjecting rats to high temperatures (40 to 42 °C) for 60 days, noticed a reduction in the size of the reproductive organs of these animals. In a study by Meade et al. (2019), heat stress induced damage to the testicular morphology, whereas older animals were more susceptible to this damage than young ones.

In this experiment, testicular morphology was not influenced by the use of different CA levels. Santos et al. (2012) found that, at 60 days of age, testicle weight stabilized at 3.59 g for meat quail and 2.49 g for laying quail. Therefore, it is believed that the animals in this study were not subjected to intense oxidative stress that would result in changes in testicular morphology.

The gonadosomatic index (GSI) was another biometric variable collected in this study. It is essential in the assessment of testicular size and is related to sperm production (Kenagy and Trombulak, 1986). In this study, the GSI did not differ among treatments (Table 2), and the average GSI in all treatments was 2.52%. Orsi et al. (2005) reported similar GSI values for Japanese quail (2.26%) and Italian quail (2.6%), whereas Lanna et al. (2013) found values for Japanese quail close to 3.7%, indicating greater sperm production capacity and storage. Therefore, light and small testicles, with a low GSI, are related to a lower reproductive capacity due to low rates of spermatogenesis and testosterone production (Santos et al., 2012).

4.2. Proteomics

The expression of equivalent bands among treatments decreased with increasing CA concentrations in the feed (Figure 2). The animal naturally produces enzymes that eliminate free radicals, which is known as the enzymatic defense system, producing enzymes such as catalase, glutathione peroxidase, and superoxide dismutase to protect the body against oxidative agents such as hydrogen peroxide, superoxide, and nitrite oxide (Ali et al., 2020). In view of this, the decrease in protein expression is believed to be due to the gradual increase in CA level as a result of the exogenous supply of antioxidant enzymes present in the feed, and therefore, the enzyme defense system does not need to produce antioxidant enzymes.

In the bands that were significantly different (Figure 2), important proteins linked to reproduction were found, such as piwi-like protein 1 (PIWL1) and heat shock protein HSP 90-alpha (HS90AA1). Of these, PIWL1 is involved in the development of the embryo and is related to spermatogenesis; its absence can therefore result in damage to germ cells during meiosis (Chen et al., 2013). The HS90AA1 is a heat shock protein (HSP) produced to protect the testis against lipid oxidation when the animal is subjected to oxidative stress, thus protecting spermatogenesis (Ohsako et al., 1995; Biggiogera et al., 1996; Grad et al., 2010).

Peroxiredoxin-6 and superoxide dismutase [Cu-Zn] (SOD1) proteins, which are important for protecting the body against ROS, were also found in this study. Peroxiredoxin-6 belongs to the class of peroxiredoxins (PRDX), which are the main antioxidant proteins of peroxides produced endogenously in eukaryotes (Han et al., 2005). According to this same author, the antioxidant activity of PRDX in chickens is similar to that found in mammals, and they are involved in the protection and repair of oxidative damage. Regarding gene ontology, this is the first mention of this protein in quail tissues, where it is closely related to the antioxidant function, testicular tissue protection, and decrease in the effects of oxidative stress on fertility.

The enzyme superoxide dismutase [Cu-Zn] plays a role in the body's defense system and neutralizes excess ROS, thus preventing damage to the cell structure (Luz et al., 2011). It naturally occurs in the testes of birds and protects them against lipid peroxidation (Mahmoodpour et al., 2017). Froman and Thurston (1981) compared SOD1 activity in the sperm of turkeys and roosters and observed that it is higher in turkey sperm than in rooster sperm. According to Mruk et al. (2002), a low SOD level in the testis would not only make the organ susceptible to oxidative damage but would also alter specific testicular functions and result in the loss of homeostasis.

The oncological results show that only 1% of the total proteins found have antioxidant function. This level is close to that reported by Słowińska et al. (2017), who studied semen of wild turkey (*Meleagris gallopavo*) and reported that of 137 proteins observed, only 2% had antioxidant function. Antioxidant activity in the testes is fundamentally important because these enzymes protect against oxidative factors, ensuring high fertility (Surai, 2002).

4.3. Histology

The seminiferous tubules of most animals have a diameter ranging from 150 to 300 μm (Razi et al., 2010). In this experiment, the lowest and highest values obtained for the diameter of the seminiferous

tubule were 183.5 and 221.3 µm, respectively. However, the values obtained in the four treatments were not influenced by the CA level used in this experiment. The heights of the germinal epithelium were significantly different according to the CA level; that is, as the CA concentration in the feed increased, the germinal epithelium shortened, resulting in faster spermatogenesis. Spermatogenesis can suffer failures due to several favors, such as nutrition, handling, and ambience. Animals subjected to heat stress, for example, may have a lower sperm concentration and motility, in addition to an affected spermatogenesis (Turk et al., 2015, 2016; Fouad et al., 2016). With the use of CA, the compounds present in it, such as carnadol, can delay the harmful effects that heat stress has on quail, resulting in increased sensitivity to steroids, which improves gamete production (Durmic and Blache, 2012).

In this study, animals in the control group had an average epithelium height of 71.2 µm, and treatment with 0.75% CA resulted in an average height of 45.6 µm. The diameter of the epididymal duct was also influenced by treatments, with a statistically significant difference between the control (29.9 µm) and the treatment with 0.75% CA (101.5 µm).

When analyzing the histological images of the testicles, we observed germ cells at different stages of development, such as spermatogonia, spermatocytes, spermatids, and spermatozoa. We also noticed the presence of Leydig cells, which are responsible for the production of testicular androgens in the interstitial space (Liu et al., 2014). Sertoli cells were also present in the seminiferous tubules of quail; they regulate germ cell development and provide energy substrates, such as lactate, and hormones (Oliveira et al., 2012). The epididymal ducts were uniform, with a high sperm presence, and efferent ducts with ciliated and non-ciliated cells. According to Franzo et al. (2008), most of the epididymis is made up of efferent ducts, which are connected to the testis network and are the sites of sperm transition to the epididymal lumen, making them fundamental for fluid absorption (Bedford, 1978; Aire, 1979).

5. Conclusions

Supplementing feed with calcium anacardate altered the expression of specific proteins of the seminal plasma of quail, in addition to facilitating histological alterations regarding the height of the seminiferous epithelium and the diameter of the epididymal duct.

Conflict of Interest

The authors declare no conflict of interest.

Author Contributions

Conceptualization: R.S. Ferreira, F.R. Vasconcelos, N.M. Vilarinho and E.R. Freitas. Data curation: R.S. Ferreira and N.M. Vilarinho. Formal analysis: R.S. Ferreira, F.R. Vasconcelos, N.M. Vilarinho and A.A.A.N. Moura. Funding acquisition: E.R. Freitas. Investigation: R.S. Ferreira, F.R. Vasconcelos, N.M. Vilarinho and E.R. Freitas. Methodology: F.R. Vasconcelos, N.M. Vilarinho, E.R. Freitas and A.A.A.N. Moura. Resources: F.R. Vasconcelos, E.C. Miguel, A.A. Calderano, L.F. Teixeira and A.A.A.N. Moura. Supervision: F.R. Vasconcelos, E.C. Miguel, E.R. Freitas and A.A.A.N. Moura. Writing – original draft: R.S. Ferreira. Writing – review & editing: F.R. Vasconcelos, E.R. Freitas, A.A. Calderano and A.A.A.N. Moura.

Acknowledgments

We would like to thank the Universidade Federal do Ceará (UFC), the Fundação Cearense de Apoio ao Desenvolvimento Científico e Tecnológico (FUNCAP), the Central Analítica of the UFC, and the Programa de Pós-Graduação em Zootecnia of the Universidade Federal de Viçosa (UFV). This work was carried out with the support of the Coordenação de Aperfeiçoamento de Pessoal de Nível Superior – Brazil (CAPES) – Financing Code 001.

References

Abreu, V. K. G.; Pereira, A. L. F.; Freitas, E. R.; Trevisan, M. T. S. and Costa, J. M. C. 2015. Addition of anacardic acid as antioxidants in broiler chicken mortadella. Food Science and Technology 35:539-545. https://doi.org/10.1590/1678-457X.6771

Aire, T. A. 1979. The ductuli efferentes of the epididymal region of birds. Journal of Anatomy 130:707-723.

Agarwal, A.; Leisegang, K.; Majzoub, A.; Henkel, R.; Finelli, R.; Panner Selvam, M. K.; Tadros, N.; Parekh, N.; Ko, E. Y.; Cho, C. L.; Arafa, M.; Alves, M. G.; Oliveira, P. F.; Alvarez, J. G. and Shah, R. 2021. Utility of antioxidants in the treatment of male infertility: clinical guidelines based on a systematic review and analysis of evidence. The World Journal of Men's Health 39:233-290. https://doi.org/10.5534/wjmh.200196

Aitken, R. J. and Roman, S. D. 2008. Antioxidant systems and oxidative stress in the testes. Oxidative Medicine and Cellular Longevity 1:15-24. https://doi.org/10.4161/oxim.1.1.6843

Ali, S. S.; Ahsan, H.; Zia, M. K.; Siddiqui, T. and Khan, F. H. 2020. Understanding oxidants and antioxidants: Classical team with new players. Journal Food Biochemistry 44:e13145. https://doi.org/10.1111/jfbc.13145

Barreiros, A. L. B. S.; David, J. M. and David, J. P. 2006. Estresse oxidativo: relação entre geração de espécies reativas e defesa do organismo. Química Nova 29:113-123. https://doi.org/10.1590/S0100-40422006000100021

Becker, J. and Craig, E. A. 1994. Heat-shock proteins as molecular chaperones. European Journal of Biochemistry 219:11-23. https://doi.org/10.1111/j.1432-1033.1994.tb19910.x

Biggiogera, M.; Tanguay, R. M.; Marin, R.; Wu, Y.; Martin, T. E. and Fakan, S. 1996. Localization of heat shock proteins in mouse male germ cells: an immunoelectron microscopical study. Experimental Cell Research 229:77-85. https://doi.org/10.1006/excr.1996.0345

Bedford, J. M. 1978. Influence of abdominal temperature on epididymal function in the rat and rabbit. American Journal of Anatomy 152:509-521. https://doi.org/10.1002/aja.1001520405

Bianchi, M. L. P. and Antunes, L. M. G. 1999. Radicais livres e os principais antioxidantes da dieta. Revista de Nutrição 12:123-130. https://doi.org/10.1590/S1415-52731999000200001

Bradford, M. M. 1976. A rapid and sensitive method for the quantization of microgram quantities of protein utilizing the principle of protein-dye binding. Analytical Biochemistry 72:248-254. https://doi.org/10.1016/0003-2697(76)90527-3

Chaturvedi, C. M. and Bhatt, R. 1990. The effect of different temporal relationships of 5-hydroxytryptophan (5-HTP) and L-dihydroxyphenylalanine (L-DOPA) on reproductive and metabolic responses of migratory red-headed bunting (*Emberiza bruniceps*). Journal of Interdisciplinary Cycle Research 21:129-139. https://doi.org/10.1080/09291019009360033

Chaturvedi, C. M.; Bhatt, R. and Phillips, D. 1993. Photoperiodism in Japanese quail (*Coturnix coturnix japonica*) with special reference to relative refractoriness. Indian Journal of Experimental Biology 31:417-421.

Chen, R.; Chang, G.; Dai, A.; Ma, T.; Zhai, F.; Xia, M.; Liu, L.; Li, J.; Hua, D. and Chen, G. 2013. Cloning and expression characterization of the chicken Piwil1 gene. Molecular Biology Reports 40:7083-7091. https://doi.org/10.1007/s11033-013-2831-9

CONCEA - Conselho Nacional de Controle de Experimentação Animal. 2015. Available at: <http://www.mct.gov.br/index.php/content/view/310553.html>. Accessed on: Dec. 20, 2018.

Costa, B. B. and Streit Jr, D. P. 2019. Estresse oxidativo e antioxidantes no de sêmen de peixes. Ciência Animal 29:93-109.

De Lazari, F. L.; Sontag, E. R.; Schneider, A.; Moura, A. A. A.; Vasconcelos, F. R.; Nagano, C. S.; Mattos, R. C.; Jobim, M. I. M. and Bustamante-Filho, I. C. 2019. Seminal plasma proteins and their relationship with sperm motility and morphology in boars. Andrologia 51:e13222. https://doi.org/10.1111/and.13222

Durmic, Z. and Blache, D. 2012. Bioactive plants and plant products: effects on animal function, health and welfare. Animal Feed Science and Technology 176:150-162. https://doi.org/10.1016/j.anifeedsci.2012.07.018

Fouad, A. M.; Chen, W.; Ruan, D.; Wang, S.; Xia, W. G. and Zheng, C. T. 2016. Impact of heat stress on meat, egg quality, immunity and fertility in poultry and nutritional factors that overcome these effects: A Review. International Journal of Poultry Science 15:81-95. https://doi.org/10.3923/ijps.2016.81.95

Franzo, V. S.; Artoni, S. M. B.; Oliveira, D.; Vulcani, V. A. S. and Sagula, A. 2008. Elétron-micrografia do epidídimo de codornas japonesas (*coturnix coturnix japonica*) em período de reprodução. Nucleus 5:173-182. https://doi.org/10.3738/1982.2278.101

Froman, D. P. and Thurston, R. J. 1981. Chicken and turkey spermatozoal superoxide dismutase: a comparative study. Biology of Reproduction 24:193-200. https://doi.org/10.1095/biolreprod24.1.193

Garrigue, M. 2017. Effet du stress thermique sur les parametres seminologiques de taureaux de centre d'insémination. Thèse d'exercice, Médecine vétérinaire, Ecole Nationale Vétérinaire de Toulouse. 61p. Available at: <https://oatao.univ-toulouse.fr/19330/1/Garrigue_19330.pdf>. Accessed on: Mar. 03, 2023.

Grad, I.; Cederroth, C. R.; Walicki, J.; Grey, C.; Barluenga, S.; Winssinger, N.; Massy, B.; Nef, S. and Picard, D. 2010. The molecular chaperone Hsp90α is required for meiotic progression of spermatocytes beyond pachytene in the mouse. Plos One 5:e15770. https://doi.org/10.1371/journal.pone.0015770

Hamad, F. B. and Mubofu, E. B. 2015. Potential biological applications of bio-based anacardic acids and their derivatives. International Journal of Molecular Sciences 16:8569-8590. https://doi.org/10.3390/ijms16048569

Han, J. Y.; Song, K. D.; Shin, J. H.; Han, B. K.; Park, T. S.; Park, H. J.; Kim, J. K.; Lillehoj, H. S. J.; Lim, J. M. and Kim, H. 2005. Identification and characterization of the peroxiredoxin gene family in chickens. Poultry Science 84:1432-1438. https://doi.org/10.1093/ps/84.9.1432

Hanafi, E. M.; Abd El Raouf, A.; Kassem, S. S.; Abdel-Kader, M. M. and Elkadrawy, H. H. 2010. A novel herbal remedy to alleviate drawbacks of heat stress in rats with special references to some reproductive and molecular alterations. Global Journal of Biochemistry and Biotechnology 5:145-152.

Kenagy, G. J. and Trombulak, S. C. 1986. Size and function of mammalian testes in relation to body size. Journal of Mammalogy 67:1-22. https://doi.org/10.2307/1380997

Kubo, I.; Masuoka, N.; Ha, T. J. and Tsujimoto, K. 2006. Antioxidant activity of anacardic acids. Food Chemistry 99:555-562. https://doi.org/10.1016/j.foodchem.2005.08.023

Lanna, L. L.; Soares, F. A.; Santos, T. M.; Oliveira, J. N. and Marques Júnior, A. P. 2013. Índice gonadossomático e correlações entre dimensões e peso testiculares na codorna japonesa (*Coturnix coturnix japonica*) aos 60 dias de idade. Arquivo Brasileiro de Medicina Veterinária e Zootecnia 65:955-960. https://doi.org/10.1590/S0102-09352013000400003

Liu, Q.; Wang, Y.; Gu, J.; Yuan, Y.; Liu, X.; Zheng, W.; Huang, Q.; Liu, Z. and Bian, J. 2014. Zearalenone inhibits testosterone biosynthesis in mouse Leydig cells via the crosstalk of estrogen receptor signaling and orphan nuclear receptor Nur77 expression. Toxicology in vitro 28:647-656. https://doi.org/10.1016/j.tiv.2014.01.013

Luz, H. K. M.; Wanderley, L. S.; Faustino, L. R.; Silva, C. M. G.; Figueiredo, J. R. and Rodrigues, A. P. R. 2011. Papel de agentes antioxidantes na criopreservação de células germinativas e embriões. Acta Scientiae Veterinariae 39:956.

Macari, M. and Maiorka, A. 2017. Fisiologia das aves comerciais. FUNEP, Jaboticabal.

Mahmoodpour, H.; Vahdatpour, S.; Jafargholipour, M. and Vahdatpour, T. 2017. Effects of low-protein diets supplemented with antioxidants on histopathology of testis and testosterone and performance of male Japanese quail (*Coturnix coturnix japonica*). Revista Brasileira de Zootecnia 46:123-129. https://doi.org/10.1590/S1806-92902017000200007

Malmir, M.; Mehranjani, M. S.; Faraji, T. and Noreini, S. N. 2021. Antioxidant effect of vitamin E on the male rat reproductive system by a high oral dose of Bisphenol-A. Toxicology Research and Application 5. https://doi.org/10.1177/23978473211005562

Meade, R. D.; Notley, S. R. and Kenny, G. P. 2019. Aging and human heat dissipation during exercise-heat stress: an update and future directions. Current Opinion in Physiology 10:219-225. https://doi.org/10.1016/j.cophys.2019.07.003

Mruk, D. D.; Silvestrini, B.; Mo, M. and Cheng, C. Y. 2002. Antioxidant superoxide dismutase - a review: its function, regulation in the testis, and role in male fertility. Contraception 65:305-311. https://doi.org/10.1016/S0010-7824(01)00320-1

Ohsako, S.; Bunick, D. and Hayashi, Y. 1995. Immunocytochemical observation of the 90 KD heat shock protein (HSP90): high expression in primordial and pre-meiotic germ cells of male and female rat gonads. Journal of Histochemistry and Cytochemistry 43:67-76. https://doi.org/10.1177/43.1.7822767

Oliveira, P. F.; Alves, M. G.; Rato, L.; Laurentino, S.; Silva, J.; Sá, R.; Barros, A.; Sousa, M.; Carvalho, R. A.; Cavaco, J. E. and Socorro, S. 2012. Effect of insulin deprivation on metabolism and metabolic-associated gene transcript levels of in vitro cultured human Sertoli cells. Biochimica et Biophysica Acta 1820:84-89. https://doi.org/10.1016/j.bbagen.2011.11.006

Orsi, A. M.; Stefanini, M. A.; Vegas, K. A. S.; Simões, K. and Antoni, S. M. B. 2005. Aspectos morfológicos do ciclo testicular anual de codorna doméstica (*Coturnix coturnix*) da variedade italiana. Brazilian Journal of Veterinary Research and Animal Science 42:163-170.

Paramashivappa, R.; Kumar, P. P.; Vithayathil, P. J. and Rao, A. S. 2001. Novel method for isolation of major phenolic constituents from cashew (*Anacardium occidentale* L.) nut shell liquid. Journal of Agricultural and Food Chemistry 49:2548-2551. https://doi.org/10.1021/jf001222j

Razi, M.; Hassanzadeh, S. H.; Najafi, G. R.; Feyzi, S.; Amin, M.; Moshtagion, M.; Janbaz, H. and Amin, M. 2010. Histological and anatomical study of the White Rooster of testis, epididymis and ductus deferens. International Journal of Veterinary Research 4:229-236.

Rostagno, H. S.; Albino, L. F. T.; Hannas, M. I.; Donzele, J. L.; Sakomura, N. K.; Perazzo, F. G.; Saraiva, A.; Teixeira, M. L.; Rodrigues, P. B.; Oliveira, R. F.; Barreto, S. L. T. and Brito, C. O. 2017. Tabelas brasileiras para aves e suínos: composição de alimentos e exigências nutricionais. 4.ed. UFV, Viçosa, MG.

Santos, T. C.; Murakami, A. E.; Oliveira, C. A. L. and Costa, P. D. 2012. Desenvolvimento corporal e testicular em machos de codornas de corte e de postura de 25 a 360 dias. Pesquisa Veterinária Brasileira 32:1205-1212. https://doi.org/10.1590/S0100-736X2012001100023

Silva, J. H. V. 2009. Tabelas para codornas japonesas e européias. 2.ed. FUNEP, Jaboticabal.

Słowińska, M.; Nynca, J.; Arnold, G. J.; Fröhlich, T.; Jankowski, J.; Kozlowski, K.; Mostek, A. and Ciereszko, A. 2017. Proteomic identification of turkey (*Meleagris gallopavo*) seminal plasma proteins, Poultry Science 96:3422-3435. https://doi.org/10.3382/ps/pex132

Snel, B.; Lehmann, G.; Bork, P. and Huynen, M. A. 2000. STRING: a web-server to retrieve and display the repeatedly occurring neighbourhood of a gene. Nucleic Acids Research 28:3442-3444. https://doi.org/10.1093/nar/28.18.3442

Souza, T. T. S.; Bezerra, M. J. B.; van Tilburg, M. F.; Nagano, C. S.; Rola, L. D.; Duarte, J. M. B.; Melo, L. M.; Moura, A. A. and Freitas, V. J. F. 2020. Protein profile of the ovarian follicular fluid of brown brocket deer (Mazama gouazoubira; Fisher, 1814). Zygote 28:170-173. https://doi.org/10.1017/S0967199419000741

Surai, P. F. 2002. Natural antioxidants in avian nutrition and reproduction. Nottingham University Press, Nottingham, Nottinghamshire.

Turk, G.; Ceribasi, A. O.; Simsek, U. G.; Ceribasi, S.; Guvenc, M.; Kaya, S. O.; Ciftci, M.; Sönmez, M.; Yüce, A.; Bayrakdar, A.; Yaman, M. and Tonbak, F. 2016. Dietary rosemary oil alleviates heat stress-induced structural and functional damage through lipid peroxidation in the testes of growing Japanese quail. Animal Reproduction Science 164:133-143. https://doi.org/10.1016/j.anireprosci.2015.11.021

Turk, G.; Simsek, U. G.; Ceribasi, A. O.; Ceribasi, S.; Kaya, S. O.; Guvenç, M.; Çiftçi, M.; Sonmez, M.; Yuce, A.; Bayrakdar, A.; Yaman, M. and Tonbak, F. 2015. Effect of cinnamon (*Cinnamomum zeylanicum*) bark oil on heat stress-induced changes in sperm production, testicular lipid peroxidation, testicular apoptosis, and androgenic receptor density in developing Japanese quail. Theriogenology 84:365-376. https://doi.org/10.1016/j.theriogenology.2015.03.035

Viana, A. G. A.; Martins, A. M. A.; Pontes, A. H.; Fontes, W.; Castro, M. S.; Ricart, C. A. O.; Sousa, M. V.; Kaya, A.; Topper, E.; Memili, E. and Moura, A. A. 2018. Proteomic landscape of seminal plasma associated with dairy bull fertility. Scientific Reports 8:16323. https://doi.org/10.1038/s41598-018-34152-w

Wang, Z. G.; Pan, X. J.; Peng, Z. Q.; Zhao, R. Q. and Zhou, G. H. 2009. Methionine and selenium yeast supplementation in maternal diets affects color, water-holding capacity and oxidative stability of the male offspring meat at the early stage. Poultry Science 88:1096-1101. https://doi.org/10.3382/ps.2008-00207